

## FUNCTIONAL DESIGN OF HORSE HOOF KERATIN: THE MODULATION OF MECHANICAL PROPERTIES THROUGH HYDRATION EFFECTS

BY J. E. A. BERTRAM\* AND J. M. GOSLINE

*Department of Zoology, University of British Columbia, Vancouver, Canada*

*Accepted 27 February 1987*

### SUMMARY

Tensile moduli and J-integral fracture toughness values were determined for horse hoof-wall keratin at four hydration levels. The stiffness of hoof-wall was influenced by water content to a greater degree than is the stiffness of other mammalian hard keratins. Young's modulus increased from 410 MPa at 100% relative hydration (RH) to 14.6 GPa at 0% RH. Fracture toughness was maximal (22.8 kJ m<sup>-2</sup>) at an intermediate hydration (75% RH), which represents a two-fold increase over both fully hydrated and dehydrated material. Maximum fracture toughness occurred at a hydration level which is within the range that has been found *in vivo* in the hoof wall. These results lead to the hypothesis that the density of secondary bonding sites within the hoof-wall keratin matrix proteins provides the hoof organ with the means to modulate tissue properties, even though this epidermal tissue functions after the cells have died.

### INTRODUCTION

The keratinous wall of the hoof transmits the forces passing between the ground and the bony skeleton of the horse. To deal effectively with these forces, the wall tissue must be sufficiently rigid to prevent excessive deformation under the imposed load. At the same time, the material must not break. Rigid materials break because they fracture; cracks originating at stress concentrations within the material grow until the material fails. Understanding the functional design of a rigid biomaterial such as hoof-wall requires understanding of both its stiffness and its fracture properties.

Deformation under an imposed load is limited in rigid composite materials, because molecular adhesion acts to resist relative movement of the material's components. The resistance to deformation of the material results from the resistance to deformation of the molecular interconnections which carry shear stress and, when deformed, develop strain energy. Resistance to deformation is termed stiffness. One consequence of increasing the stiffness of materials is usually a

\*Present address: Department of Anatomy, University of Chicago, Chicago, IL 60637, USA.

Key words: keratin, fracture, hydration effects.

reduction of fracture resistance that causes the material to become more brittle. This occurs because the intercomponent connections within the material, as well as bearing shear stress, are also able to communicate stresses around flaws or discontinuities. This allows applied force to become concentrated as high stresses at the end of the flaw. These localized stress concentrations jeopardize the material by reducing the total energy required to cause fracture (Griffith, 1921).

The properties of keratinous materials are strongly influenced by their hydration state. Studies on several hard keratin structures indicate that stiffness is inversely related to hydration level in these materials (Fraser & MacRae, 1980). Since the stiffness of a material can influence its fracture behaviour, the hydration state may be an important factor in determining the resistance to fracture, or toughness, of exposed rigid keratins, such as the equine hoof-wall. In this study we investigate the relationship between stiffness and toughness in horse hoof-wall keratin and the role hydration plays in determining these two properties in this material.

The hoof-wall is a unique constituent of the supporting limb. Like all epidermal tissues the hoof-wall is avascular; fluids and nutrients are supplied by diffusion through a basal membrane lying in contact with the vascularized dermis. Epidermal tissues are completely cellular. The mechanical properties of hoof-wall are dependent on the epidermal cells and their geometric organization, rather than on an extracellular framework as in the other stiff skeletal biomaterials (such as bone).

Epidermal cells synthesize a diverse group of proteins, called keratins, that are laid down within the cell. Keratin is a protein composite consisting of two phases: a fibre phase mainly constructed from long slender  $\alpha$ -helical microfibrils, which is cross-linked to an amorphous protein matrix phase (Fraser & MacRae, 1980). The cells responsible for keratin synthesis, termed keratinocytes, die in the final stages of their differentiation when disulphide cross-links are established in the keratin proteins within their cytoplasm. The extensive molecular cross-linking within the keratin produces a stable composite of long, thin fibres embedded in a surrounding matrix.

The keratin cells of the hoof-wall are subject to various hydration conditions. Hydrating fluids originate within the dermis underlying the epidermal wall, except when the animal is actually standing in water. These fluids are lost through all external surfaces of the hoof. As a consequence, two hydration gradients normally exist within the hoof. A horizontal gradient, in which the outer surfaces of the hoof have low hydration levels while the interior, adjacent to the dermis, maintains a high hydration level, and a vertical gradient in which hydration decreases from the proximal germinative region to the distal contact surface (Fig. 1).

Hoof keratin is produced by the division of cells in the narrow germinative region at the proximal border of the wall. Consequently, it cannot regenerate or remodel *in situ* because the keratinocytes from which it is derived die in the final stages of their differentiation. Thus, all required material properties must be anticipated through structural design at the time of tissue deposition. However, both the properties provided by the keratin cells and the mechanical environment to which they are subjected vary during the period these cells reside in the wall (approximately 1 year). In this study, we show that the response of hoof-wall keratin to the various hydration

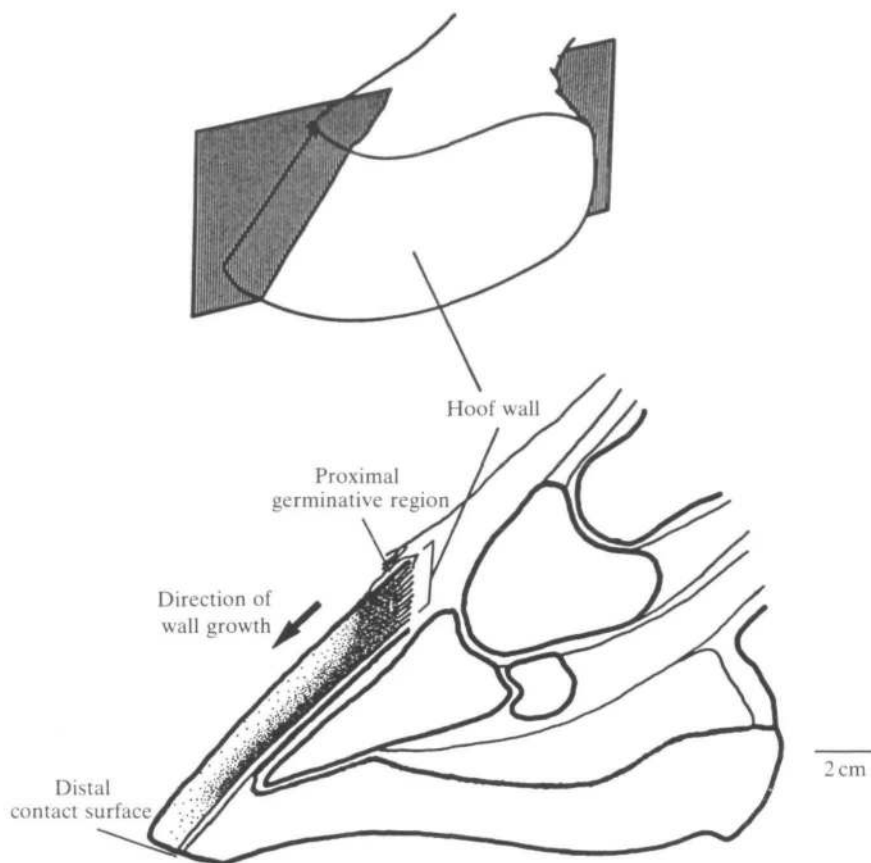


Fig. 1. Sagittal section of hoof wall, plane of section shown above. Hydration gradients indicated by density of stippling in lower diagram. Wall grows from germinative region at upper right (which includes dermal papillae) towards distal contact surface at base of hoof wall.

levels present in the hoof provides a mechanism through which the mechanical properties of this tissue can be modulated and matched to the functional requirements of the animal.

#### MATERIALS AND METHODS

##### *Morphology and specimen preparation*

The test specimens were removed from the central epidermal layer (*stratum medium*) of the anterior face of the hoof-wall of freshly killed, adult horses obtained from a local abattoir. The majority of hoof-wall is composed of *stratum medium* and it is this tissue that makes up the externally visible wall, except for a thin layer at the proximal border (the *stratum externum*). The *stratum medium* is produced at the proximal border of the wall and grows distally until it is worn away at the ground contact surface (Fig. 1). It is composed of keratin cells organized into two distinct patterns. Approximately half of the hoof-wall keratin cells are produced on dermal

papillae and form what have become known as tubules (Nickel, 1938; Wilkens, 1964; Leach, 1980; Bertram & Gosline, 1986). The tubules run from the proximally positioned dermal papillae, parallel to the external surface of the wall, until they reach the distal contact surface. The cells of the tubules are broad and flattened around the circumference of the tubule. Together these cells form a hollow-centred cylinder with fibres organized in a steep spiral pattern winding around the tubule axis and displaying a roughly alternating spiral direction from layer to layer. The remaining wall material is produced on the basal epidermal membrane between the dermal papillae. These cells are also broad and flattened, but have their longest axis roughly parallel to the distal contact surface and form a series of planes of parallel-fibred material running between the more vertically oriented tubules. The influence of this organization on the mechanical properties has been discussed previously (Bertram & Gosline, 1986).

To evaluate the role of hydration level, the test pieces were equilibrated at four hydration levels. Full hydration was produced either by placing the test samples over distilled water in environment-controlled test chambers or by immersion. The water content of samples was determined by measuring the mass loss of oven-dried specimens (80°C, 5 days). The samples were dehydrated by being placed over phosphorous pentoxide drying agent (BDH Laboratories). Intermediate hydration conditions of 53% RH and 75% RH were produced by placing the test specimens over saturated solutions of  $\text{Mg}(\text{NO}_3)_2 \cdot 6\text{H}_2\text{O}$  and NaCl in the environment test chambers (Meites, 1963). The design of the environment test chambers allowed the fracture testing of samples within the constant-humidity environment.

Tensile tests were conducted using an Instron Model 1122 tensile testing machine with a 500-kg load cell and an extension rate of  $5 \text{ mm min}^{-1}$ . These tests used strips of hoof-wall with dimensions of approximately 0.6 mm (thickness)  $\times$  4 mm (width)  $\times$  2.5 cm (length). The test samples were taken from the same region of the hoof-wall as the fracture samples and were oriented with the tubule axes parallel to the tension load (Fig. 2). The specimens were allowed to equilibrate at the four hydration levels and were tested immediately after removal from equilibration chambers. The samples were clamped above and below using pneumatic sample grips. To eliminate end-effects caused by sample gripping, strain was measured by following the movement of surface fiducial marks placed away from the sample grips, using a video dimension analyser (Model 303, Instruments for Physiology & Medicine, La Jolla, CA, USA). Initial Young's modulus ( $E$ ) was determined from the maximum slope (linear region) of the tensile stress (force/area) *vs* strain (loaded/original length) records.

Fracture tests were carried out using the compact tension test geometry. Blocks were removed from the hoof-wall and machined to the compact tension (CT) test configuration as described previously (Bertram & Gosline, 1986). In this study, the CT specimens were formed with the pre-cut notch oriented parallel to the direction of the tubular axis of the material (Fig. 2). Thus, the test attempts to drive the crack in what would be the proximal direction in the intact hoof, the direction of greatest fracture toughness (Bertram & Gosline, 1986). Fracture toughness values were

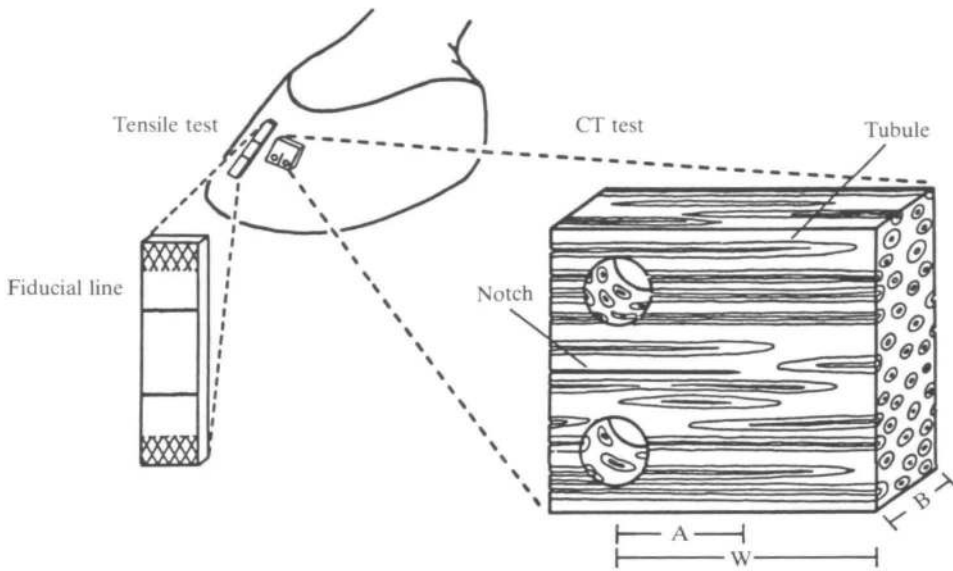


Fig. 2. Location and orientation of longitudinal tension and compact tension (CT) test specimens. Cross-hatched region on tensile specimen indicates pneumatic grip location. Compact tension: A, notch length; W, specimen width; B, specimen thickness. Note: expanded drawings of tensile and compact tension specimens are not to the same scale.

determined by the J-integral method of Rice (1968), as adapted for this material (Bertram & Gosline, 1986).

Toughness is a measure of the resistance to the growth of flaws. The growth of flaws (in the form of microscopic cracks), or fracture when the condition reaches a critical state, is dependent on the formation of new surfaces within the material. The formation of new surfaces requires energy. A thorough analysis of the circumstances in which a material fractures requires a measure of the energy necessary for crack growth. The J-integral is a measure of the instantaneous change in energy with an incremental change in crack length at the critical point of failure. For a given specimen the critical J-integral value ( $J_{crit}$ ) was evaluated by plotting the energy ( $U$ ) against the apparent crack length ( $a$ ) (this value is derived from the mechanical test record using the calibration curve – see description in Results) to specimen width ( $W$ ) ratio for each interval of extension (all data together produced a series of incremental curves). The derivative of this relationship was taken at the critical failure point (critical failure was defined as the point on the force/deflection curve that intersected a line from the origin of the test having a slope which was 5% less than the maximum slope). Thus, the J-integral is defined by Broek (1978) as:

$$J = (-1/B) \times (\partial U / \partial a)_q,$$

where  $B$  is the specimen width [the term  $(-1/B)$  is included to normalize for small width variations] and  $q$  is the test machine cross-head extension (the extension at the point of critical failure is used to determine the values of  $U$  and  $a$  appropriate for calculating the critical  $J$  value).

## RESULTS

*Hydration properties*

Hoof-wall keratin samples equilibrated with a 100% RH environment were found to have a  $40.2\% \pm 2.7$  (S.D.) ( $N=24$ ) water content by mass. Relative humidity levels of 75% and 53% produced water content values of  $18.2\% \pm 0.3$  ( $N=12$ ) and  $11.7\% \pm 2.7$  ( $N=18$ ), respectively. Periods of 2–3 weeks in 0% RH produced specimens which had a consistent apparent water content of  $5.5\% \pm 1.8$  ( $N=24$ ) by mass, as indicated by oven drying. It is expected that a period of this length in 0% RH would remove all water from this material. The loss of mass observed probably represents a loss of very tightly bound water or, less likely, of some other volatile component of the tissue. The hydration values presented in this study are given as measured in order to allow direct comparison with previous studies employing the same techniques for determining *in vivo* hydration. The relationship between environmental humidity and hoof keratin water content, the absorption isotherm, is given in Fig. 3.

*Tensile tests*

The tensile properties of hoof-wall are profoundly influenced by the hydration conditions of the test specimens (Table 1). The mean Young's modulus value was found to be 410 MPa for longitudinal samples tested at 100% RH. The stiffness increased as the hydration level was decreased. The mean modulus became 2.6 GPa

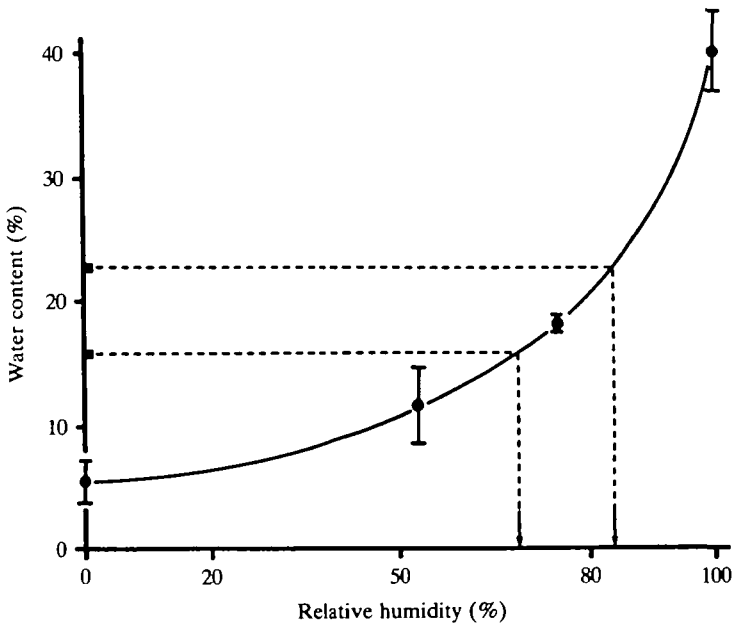


Fig. 3. Absorption isotherm for hoof-wall keratin. Relative humidity produced as described in text. Error bars indicate standard deviation around the mean. Dotted lines indicate range of normal *in vivo* water content (17–24%) as determined by Leach (1980) and arrows indicate the corresponding RH values.

Table 1. Longitudinal tensile modulus ( $E$ ) and yield stress in horse hoof-wall keratin at four relative humidity levels (RH)

RH (%)	$E$ (GPa)	s.e.	Yield stress (MPa)		$N$
				s.e.	
100	0.410	0.032	9.18	0.42	19
75	2.63	0.362	38.9	4.70	5
53	3.36	0.629	—	—	2
0	14.6	0.071	—	—	2

s.e., standard error;  $N$ , sample number. Cross-head displacement rate,  $5 \text{ mm min}^{-1}$ .

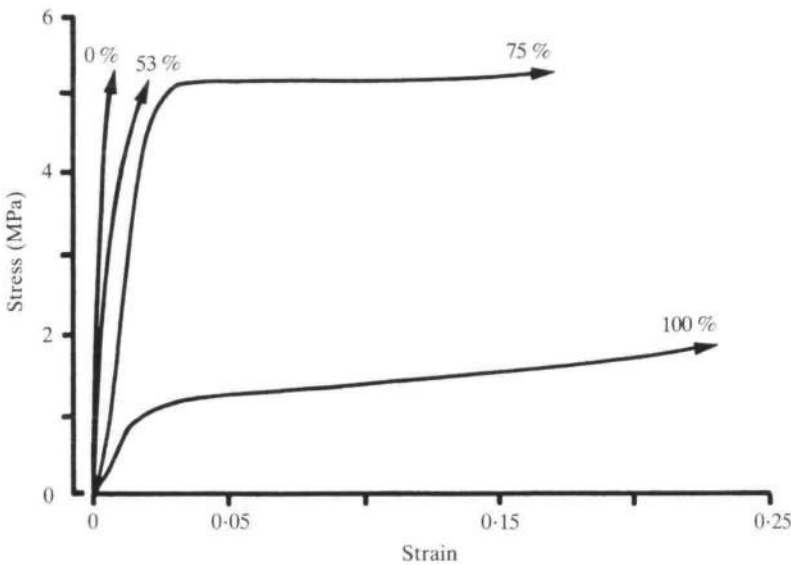


Fig. 4. Representative tensile tests stressed parallel to the tubule axis at four hydration levels. Arrowheads indicate test specimens failed at sample grips and absolute strength was not measured.

at 75% RH and 3.4 GPa at 53% RH. The greatest mean modulus, 14.6 GPa, was reached at 0% RH.

A comparison of the stress-strain behaviour of representative tensile samples (Fig. 4) indicates both a general increase in stiffness with decreased hydration and a decrease in maximum extensibility. At higher hydration levels, hoof-wall keratin behaves much as other hard keratins, displaying an initial linear elastic range after which yield occurs. At 100% RH, strains of between 0.25 and 0.30 were achieved, and failure generally occurred at the test grips. For this reason the absolute strength or extensibility could not be measured. Use of the video measurement system, however, ensured that stiffness was determined accurately. Stress levels were maintained in the post-yield region and some strain hardening behaviour was seen.

At hydration levels of 53% and 0% RH, little or no yield was seen and the material fractured in a brittle fashion. This occurred, however, at stress levels several times

Table 2. *Compact tension-fracture test results according to hydration level*

Relative humidity (%)	$J_{crit}$ ( $\text{kJ m}^{-2}$ )	S.E.	<i>N</i>
100	11.93	0.90	30
75	22.82	0.31	16
53	5.63	0.54	28
0	8.73	0.97	16

$J_{crit}$ , mean critical J integral.

greater than the yield stress of the fully hydrated material. At 75 % RH, high stress levels were achieved prior to yield, while strains of up to 0.15 were also seen. The combination of high yield stress and high strain indicates that a great deal of energy can be absorbed by this material at 75 % RH. This observation was confirmed by the fracture mechanics tests which follow.

#### *Compact tension fracture tests*

##### *Compliance calibration*

The resistance provided by a compact tension specimen against a load which tends to open the notch will depend, all other factors being equal, on the length of the notch. Standardized specimen size and shape allows quantification of the influence of notch length on the force required to deform the specimen (which is known as the mechanical compliance). A calibration curve can then be produced relating these two factors. Using the compliance calibration curve, the mechanically apparent length of the crack in a fracturing specimen can be determined from the fracture test record (in which applied load and the resulting deformations are measured). This technique is employed in the study of materials which display complex fracture behaviour. A complex fracture path eliminates the possibility of visual measurement of crack length.

The compliance value determined for a given notch length and specimen size will depend on the stiffness of the material. Since hoof-wall stiffness is dependent on hydration level, four compliance calibration relationships were determined to fit the four hydration levels used in this study. At 100 % RH, the raw data were best described by a third-order polynomial regression over the range of notch lengths used in this study ( $P < 0.001$ ;  $r^2 = 0.88$ ). Less extensive compliance calibration curves were used for the lower hydration levels, since the range of notch lengths employed was also less extensive. These relationships were best described by linear regressions over this range (Fig. 5). All regressions were significant (75 % RH,  $P < 0.025$ ; 53 % RH,  $P < 0.025$ ; 0 % RH,  $P < 0.01$ ).

##### *Fracture toughness*

The mean value of the J-integral at the critical failure point ( $J_{crit}$ ) reached a maximum at 75 % RH ( $22.8 \text{ kJ m}^{-2}$ , Table 2). This value was significantly different from those at all other hydration levels [Tukey's *w*-procedure, Tukey (1951);  $P < 0.05$ ]. The mean value of  $J_{crit}$  at 100 % RH ( $11.9 \text{ kJ m}^{-2}$ ) was significantly



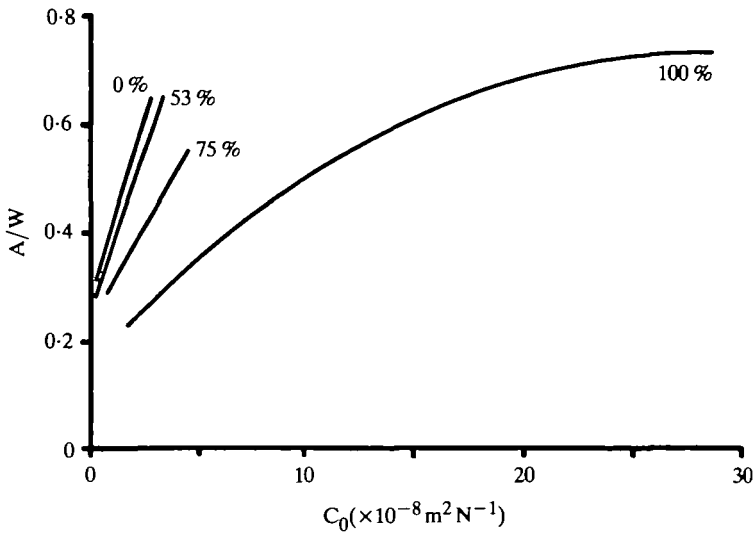


Fig. 5. Compliance calibration curves used to determine apparent crack length ( $a$ ) for the four hydration levels tested. Initial compliance value ( $C_0$ ) on the abscissa and notch length ( $A$ ) to specimen width ( $W$ ) ratio ordinate.

100% RH:  $A/W = 0.21196119 + 3.4139645 \times 10^6 C_0 - 6.652877 \times 10^{12} C_0^2 + 4.118235 \times 10^{18} C_0^3$  ( $P < 0.001$ ).

75% RH:  $A/W = 0.23706 + 7.18884 \times 10^6 C_0$  ( $P < 0.025$ ).

53% RH:  $A/W = 0.257563 + 1.20914 \times 10^7 C_0$  ( $P < 0.025$ ).

0% RH:  $A/W = 0.282584 + 1.32607 \times 10^7 C_0$  ( $P < 0.010$ ).

different from that at 53% RH ( $5.6 \text{ kJ m}^{-2}$ ) but could not be distinguished statistically from the 0% RH value ( $8.7 \text{ kJ m}^{-2}$ ). The mean values at 53% and 0% RH also could not be distinguished from each other statistically.

## DISCUSSION

### *Stiffness*

A comparison of stiffness properties of hoof-wall with other keratinous materials indicates that the tensile response of hoof keratin to dehydration is generally similar to that of other keratins (Table 3). However, the level of water content has a more dramatic effect on the tensile properties of hoof-wall keratin. To understand how this can occur it is necessary to view the material at the level of its molecular composition and organization.

Fraser & MacRae (1980) have pointed out that, even within the mammals, the term keratin includes a diverse range of epidermal intracellular proteins. These can be divided into two groups based mainly on protein composition. Those termed 'soft' keratins, such as are found in the *stratum corneum* (skin) of mammals, are composed of microfibrils with both  $\alpha$ -helical and non-helical domains, and these are embedded in a matrix of two varieties of protein, one rich in disulphide cross-linking cysteinyl residues and the other rich in histidiny residues (Matoltsy, 1975; Dale, 1977; Jones, 1980). Epidermal appendages, such as horn, hair, claws and hooves, contain 'hard'

Table 3. *Longitudinal elastic moduli (stiffness) of keratinized structures and the effect of hydration level (in GPa) (after Fraser & MacRae, 1980)*

	Relative humidity			Reference
	0%	Intermediate (RH in parentheses)	100%	
Human nail		2.6 (70%)	1.8	1
hair		2.3 (70%)	1.5	1
stratum corneum		0.19 (70%)	0.13	1
Wool	5.6		2.0	2
Horsehair	6.8	5.1 (60%)	2.4	3
Hoof wall	14.6	3.36 (53%)    2.6 (75%)	0.41	

1. Baden, Goldsmith & Lee (1974). 2. Meredith (1956). 3. Bendit (1976).

keratin. Again, in this case the microfibrils possess both  $\alpha$ -helical and non-helical domains. However, unlike that of soft keratins, the non-helical microfibril domain of hard keratins is rich in cysteinyl residues. The matrix of hard keratins possesses cysteine-rich protein similar to that found in soft keratin, and in addition contains a protein rich in glycine and tyrosine. The  $\alpha$ -helical portions of the microfibrils are crystalline and can be considered to be quite stable, especially considering that the microfibrils of keratin are composed of several  $\alpha$ -helical chains formed into coiled-coil rope-like structures, reducing the sites available for intermolecular reactivity (McLachlan, 1978). In hard keratins, cysteine-cysteine disulphide cross-links stabilize the non-helical domains of the microfibrils and the cysteine-rich proteins of the matrix. The remainder of the matrix, however, has few covalent cross-links and, therefore, its stabilization depends on secondary cross-linking mechanisms which may be hydration-dependent (e.g. hydrogen bonding).

Thus, we might predict that hydration changes will more strongly affect the properties of the matrix phase than the microfibrillar phase. The structural complexity of the keratin in the equine hoof-wall, which involves tubular and intertubular components each with different fibre orientations, makes it difficult to test this prediction. Wool, however, has a simpler structure with all microfibrils oriented roughly parallel to the axis of the wool fibre. As a consequence, wool behaves as a simple parallel-fibre composite, and changes in mechanical properties with hydration can be used to assess the effect of hydration on the matrix and microfibrils. The drying of wool fibres increases the tensile modulus approximately three-fold, but increases the torsional modulus by a factor of 15 (Feughelman, 1959). The relatively small change in tensile modulus indicates that the microfibrils which carry the majority of the stress in this direction (the strand acts as a parallel composite in which the components are subject to equal *strain*) are only slightly affected by decreased hydration. However, the large change in torsional modulus indicates that the matrix properties are strongly affected by hydration level. In torsion, a large proportion of the stress applied will be carried by the matrix between the microfibrils (the wool strand loaded in this manner acts as a series composite and both components experience a far more equal *stress*). It can be concluded, then, that

dehydration affects the properties of the matrix to a far greater degree than it does the microfibrils (Fraser & MacRae, 1980). Extensive hydrogen bonding between polymers of the matrix phase in the absence of water has been described as the cause of these changes (Fraser & MacRae, 1980). These may well occur associated with the glycine/tyrosine-rich proteins found in the hard keratin matrix. Such secondary cross-linking would decrease the mobility of the matrix polymers and, in the fully dehydrated state, the matrix would become a 'rigid polymeric glass' and the stiffness would approach that of the crystalline microfibrils.

Alternatively, when keratin is highly hydrated, the matrix lacks much of the secondary bonding it possesses in the dry state. In this case, longer distances occur between cross-link positions giving the matrix polymers greater freedom of movement. This translates into lower stiffness, since the secondary cross-links are not available to carry load, and greater extensibility, due to the ability of the polymers to rearrange under load.

### Fracture

Rigid structural materials, man-made or natural, generally fail at load levels far below their ultimate theoretical strength because localized stress levels around flaws or cracks can be much greater than the general stress and can lead to crack growth and fracture. For this reason, fracture behaviour is important in determining the functional limitations of a material such as hoof-wall keratin. Over the complete range of hydrations, hoof-wall keratin proved to be a remarkably fracture-resistant material. The lowest mean work of fracture,  $5.6 \text{ kJ m}^{-2}$  at 53% RH (measured using the J-integral method), is roughly twice or more the toughness value measured for fresh bone ( $1.0\text{--}3.0 \text{ kJ m}^{-2}$  measured as strain energy release rate, Wright & Hayes, 1977). Under the optimum conditions (i.e. 75% RH), the toughness of hoof-wall keratin ( $22.0 \text{ kJ m}^{-2}$ ) is an order of magnitude greater than that of bone and even exceeds that of wood ( $10.0 \text{ kJ m}^{-2}$ ), an extremely tough biomaterial (Jeronimidis, 1976).

An indication of the significance of fracture toughness in a material such as hoof-wall can be seen by estimating the critical flaw size ( $a_f$ ) or its 'notch sensitivity'. Critical flaw size is a concept developed by Griffith (1921) and emerged from an understanding of the energy balance within a fracturing material. Fracture in a stressed material will be spontaneous when the energy released from the material surrounding a growing crack is equal to the energy required to form new surfaces (i.e. the crack surfaces). For the critical failure stress, the maximum stress a material is capable of withstanding before fracture occurs, a minimum critical flaw size exists in which spontaneous fracture will begin. The fracture criterion for a linearly elastic material is given by:

$$a_f = \frac{2E(\gamma_s + \gamma_f)}{\sigma_c^2},$$

where  $E$  is Young's modulus of elasticity,  $\sigma_c$  is critical failure stress,  $\gamma_s$  is surface energy and  $\gamma_f$  is the work of fracture, a term which incorporates energy absorbed

through several processes such as heat dissipation, plastic deformation and fibre pull-out. For most materials  $\gamma_f$  is several orders of magnitude greater than  $\gamma_s$  so  $a_f$  can be estimated by:

$$a_f = \frac{2E\gamma_f}{\sigma_c^2}.$$

As an example of a notch-sensitive material we can look at a very familiar structural biomaterial, bone. Young's modulus ( $E$ ) for fresh bone is approximately 20 GPa (Wainwright, Biggs, Currey & Gosline, 1982), yield stress ( $\sigma_y$ ) is 200 MPa (Reilly & Burstein, 1975) and strain energy release rate ( $G_{Ic}$ ) is  $2.0 \text{ kJ m}^{-2}$  (Wright & Hayes, 1977). It has been determined that  $2\gamma_f = G_{Ic}$  (ASTM, 1965), where  $G_{Ic}$  is the strain energy release rate at failure in the opening mode. The critical flaw size is, therefore, in the range of  $300 \mu\text{m}$ . This figure indicates that any flaw greater than  $300 \mu\text{m}$  in a bone will cause failure when load is applied. Currey (1962) has discussed the design features of bone that help avoid stress concentrations due to such features as the lacunae around osteocytes and the canals for the penetration of blood vessels. Hoof-wall keratin, however, is a very notch-insensitive material. For linear elastic conditions,  $J_{crit} = G_{Ic}$  (Parker, 1981). Critical flaw size can then be estimated by:

$$a = \frac{EJ_{crit}}{\sigma_y^2},$$

where  $\sigma_y$  is yield stress. At 100% RH,  $E = 4.1 \text{ MPa}$ ,  $J_{crit} = 8.7 \text{ kJ m}^{-2}$  and  $\sigma_y = 10 \text{ MPa}$ . Therefore, under these conditions the critical flaw size for a catastrophic rupture would be about 1.5 m, a value which is more than an order of magnitude larger than the entire hoof. These, admittedly rough, calculations indicate that, even with a large margin for error, no critically sized crack can exist in the hoof-wall, and it is virtually impossible for catastrophic fracture to occur. The high toughness level (i.e. extreme notch insensitivity) at 100% RH arises from the considerable plasticity that the material displays. By deforming plastically around a stress concentration, the stress is distributed to material farther from the crack tip and greater energy is absorbed. Flaws, such as the test notch introduced into these specimens, are not critical stress concentrators at very high hydration levels because the interconnections between the phases of the composite do not carry stress well. The result, however, is a material with a relatively low yield stress, and therefore it is not capable of supporting loads as large as it could if it were dryer.

Decreasing hydration will increase the stiffness of hoof-wall keratin, but in many materials an increase in stiffness can adversely affect the notch sensitivity and fracture properties, making them brittle. Even at the lowest hydration levels (50 and 0% RH), hoof keratin retained substantial fracture toughness. This is not surprising considering its structural complexity. The interfacial surfaces between the fibre and matrix phases of a composite can provide resistance to crack growth even when both components are stiff. Energy is absorbed by separating the two phases of the composite as the growing crack approaches (Cook & Gordon, 1964). In hoof-wall, this phenomenon can occur at the level of the microfibrils and matrix of the keratin

itself, at cell boundaries within the tissue, and at the level of the tubular and intertubular components (Bertram & Gosline, 1986).

Conditions are appropriate within most of the thickness of the wall to provide the structural integrity the supporting wall requires. A reasonably high degree of rigidity is required of the hoof-wall material, but this rigidity must be balanced with the ability to resist fracture. Hoof-wall keratin at 75 % RH exhibited reasonable stiffness combined with both high yield stress and extensibility. This situation resulted in the maximum energy absorption, and hence fracture resistance, as determined through the J-integral analysis. These results are most probably the result of an intermediate degree of secondary cross-linking that increases the stiffness of the matrix phase while still allowing some extensibility. Thus, an intermediate degree of secondary cross-linking increases the fracture resistance of this material. Leach (1980) found that the major portion of the wall midway between the internal and external surfaces possessed water contents of between 17 and 24 % by mass. This is in the same range determined for the 75 % RH tested in this study [ $18.2\% \pm 0.3$  S.D. ( $N = 12$ ); Fig. 3]. Thus, hoof-wall keratin appears to function *in vivo* at the hydration levels that closely match the optimum condition for fracture toughness. In spite of the notch insensitivity displayed by this material, horse hooves do occasionally crack, probably because of a combination of decreased hydration near the external surface and long-term use causing the fracture toughness to decrease. A decline in fracture toughness by approximately 50 % has been reported for the most distal, and consequently the oldest, portions of the hoof-wall (Bertram & Gosline, 1986).

#### *Hoof wall design*

Given that hoof-wall keratin functions under hydration conditions which maximize fracture resistance, the question arises: is this an aspect of the mechanical design of this particular biomaterial, or simply a fortuitous result of the hydration conditions which exist in this circumstance? The answer can be suggested by determining whether or not hoof-wall keratin differs from other hard keratins, and if so, whether the differences reflect an adaptation of this biomaterial to the physical circumstances of the functioning hoof.

The effects of humidity on the tensile stiffness of several epidermal materials (Table 3) indicate that hoof-wall keratin displays a similar but more exaggerated increase in uniaxial stiffness with decreased hydration. Stiffness in hoof-wall keratin changes over a range 10 times greater than that for any other mammalian hard keratin material for which this property has been measured. Compared to wool, hoof-wall keratin has approximately one-fifth the stiffness at full hydration and has over 2.5 times the stiffness when dehydrated. These differences are undoubtedly due in large part to the complex structure of hoof-wall, which contains tubules and intertubular material the other materials do not possess. But, in addition, it is likely that differences in keratin protein composition contribute as well. The 15-fold change in torsional stiffness seen for wet and dry wool suggests that the matrix stiffness may increase by 15 times when wool is dehydrated. If hoof-wall keratin contains similar matrix proteins, it is likely that the increase in stiffness with dehydration would be no

more than 15-fold, and probably considerably less because of the complex organization. The 30-fold increase in overall stiffness and the variation in relative stiffness with hydration when compared to wool strongly suggest that the matrix proteins in hoof-wall keratin have an increased potential for secondary bonding relative to other hard keratins such as wool. Just the proper amount, in fact, to provide the maximum fracture resistance within the hydration conditions that normally exist in the hoof. This effect could be derived either from an adjustment in the concentration and organization of amino acid residues within the matrix proteins or from an adjustment in the proportion of the two matrix protein types, if one is indeed more sensitive to hydration effects than the other. Whether or not horse hoof keratin represents a case of molecular adaptation which provides for the complex suite of mechanical properties displayed by this tissue will depend on the results of comparative analysis of matrix protein composition data from various types of hard keratins, including hoof-wall.

The effect of hydration on the mechanical behaviour of hoof keratin and the hydration gradient found *in vivo* in the hoof-wall provide a mechanism through which the mechanical properties of different areas of the hoof-wall can be adjusted to the requirements of the hoof, in spite of the fact that this material is not alive. This can occur because both the mechanical requirements of the hoof organ and the hydration level are closely associated with specific locations within the wall. It has been shown that the *stratum medium*, which comprises the majority of the wall, has properties that are capable of providing both support and fracture resistance under the hydration conditions found in that region. The properties measured at other hydration levels also match the requirements that can be expected to occur within the regions of the wall where those hydration conditions are found.

The hoof keratin located on the interior surface, next to the basal membrane and living cell layer, is highly hydrated. Under these conditions it would be far less stiff than in drier areas and also capable of extensive plastic deformation, as is seen in the tensile tests performed at 100% hydration (Fig. 4). The living layer of epidermal cells at the basal membrane is able to transfer the impact load from the hoof-wall to the collagenous connections of the dermis during ground contact simply because three-dimensional interdigitations at the dermal/epidermal boundary increase the area of contact and distribute the load, reducing stress levels (Stump, 1967). Extensibility of the fully keratinized tissue in this area, provided for by the properties of hoof-wall keratin at this hydration level, would also ensure that the stresses were low and distributed evenly across the basal membrane and the vulnerable living cell layer. The fibre organization also differs slightly in this region, which is likely to add to this effect.

At the external surfaces, the outer face of the hoof and the distal contact surface, the hoof keratin will be equilibrated with the external environment. Under most conditions, this means the tissue will be relatively dehydrated and can be expected to be very rigid. At these locations, a hard, abrasion-resistant covering would protect against puncture and abrasive wear.

The hydration environment of the individual cells also changes during the course of their function. Cells produced at the proximal margin of the wall migrate distally as new cells are produced next to the epidermal basal membrane. Even though they are fully keratinized soon after being produced, the high hydration level makes the cells next to the germinative layer quite pliable, again protecting the vulnerable underlying tissue such as that on the attachment surface of the internal wall. These same cells eventually become the cells of the main portion of the wall and finally become contact surface material before being worn away (Fig. 1). As the cells move distally, their hydration state and their properties change.

Intracellular deposition of keratin and the subsequent death of the cells necessarily restricts the manner in which this tissue can be modified during its use. The complex structure of the hoof wall, however, requires that a material be used which has variable mechanical properties. It appears the solution to this problem has been found in the linking of hydration-dependent mechanical properties to the pattern of hydration which exists within the hoof wall.

## REFERENCES

- ASTM (1965). Fracture toughness testing and its applications. STP 381. Philadelphia.
- BADEN, H. P., GOLDSMITH, L. A. & LEE, L. (1974). The importance of understanding the comparative properties of hair and other keratinized tissues in studying disorders of hair. In *The First Human Hair Symposium* (ed. A. C. Brown), pp. 388–398. New York: Medicom.
- BENDIT, E. G. (1976). Longitudinal and transverse mechanical properties of keratin in compression. In *Proceedings of the Fifth International Wool Textile Research Conference*, vol. 2 (ed. K. Ziegler), pp. 351–360. Aachen: Deutsches Wolforschungsinstitut.
- BERTRAM, J. E. A. & GOSLINE, J. M. (1986). Fracture toughness design in horse hoof keratin. *J. exp. Biol.* **125**, 29–47.
- BROEK, D. (1978). *Elementary Engineering Fracture Mechanics*. The Netherlands: Sitjthoff & Noorhoff International Publishers.
- COOK, J. & GORDON, J. E. (1964). A mechanism for the control of cracks in brittle systems. *Proc. R. Soc. Ser. A* **282**, 508–520.
- CURREY, J. D. (1962). Stress concentrations in bone. *Q. Jl microsc. Sci.* **103**, 111–133.
- DALE, B. A. (1977). Purification and characterization of a basic protein from the stratum corneum of mammalian epidermis. *Biochim. biophys. Acta* **491**, 193–204.
- FEUGHELMAN, M. (1959). A two-phase structure for keratin fibres. *Text. Res. J.* **29**, 223–228.
- FRASER, R. D. B. & MACRAE, T. P. (1980). Molecular structure and mechanical properties of keratins. In *The Mechanical Properties of Biological Materials. Symp. Soc. exp. Biol.* **XXXIV** (ed. J. F. V. Vincent & J. D. Currey), pp. 211–246.
- GRIFFITH, A. A. (1921). The phenomena of rupture and flow in solids. *Phil. Trans. R. Soc. Ser. A* **221**, 163–198.
- JERONIMIDIS, G. (1976). The fracture of wood in relation to its structure. In *Wood Structure in Biological and Technological Research* (ed. P. Baas, A. J. Bolton & D. M. Catling), Leiden Botanical Series no. 3, pp. 253–265. Leiden: The University Press.
- JONES, L. N. (1980). Protein composition of mammalian stratum corneum. In *Fibrous Proteins: Scientific, Industrial and Medical Aspects*, vol. 2 (ed. D. A. D. Parry & L. K. Creamer), pp. 167–175. New York: Academic Press.
- LEACH, D. H. (1980). The structure and function of equine hoof wall. Ph.D. thesis, Department of Veterinary Anatomy, University of Saskatchewan, Saskatoon, Saskatchewan, Canada.
- MCLACHLAN, A. D. (1978). Coiled-coil formation and sequence regulations in the helical regions of  $\alpha$ -keratin. *J. molec. Biol.* **124**, 297–304.
- MATOLTSY, A. G. (1975). Desmosomes, filaments and keratohyaline granules: their role in stabilization and keratinization of the epidermis. *J. invest. Derm.* **65**, 127–142.

- MEREDITH, R. (1956). *The Mechanical Properties of Textile Fibres*. Amsterdam: North-Holland.
- MEITES, L. (1963). *Handbook of Analytical Chemistry*. Toronto: McGraw-Hill.
- NICKEL, R. (1938). Über den Bau der Hufrohren und seine Bedeutung für den Mechanismus des Pferdehufes. *Dt.-öst. tierärztl. Wschr.* **46**, 449–552.
- PARKER, A. P. (1981). *The Mechanics of Fracture and Fatigue. An Introduction*. London: E. & F. N. Spon Ltd.
- REILLY, D. T. & BURSTEIN, A. H. (1975). The elastic and ultimate properties of compact bone tissue. *J. Biomech.* **8**, 393–405.
- RICE, J. R. (1968). A path independent integral and the approximate analysis of strain concentration by notches and cracks. *J. appl. Mech.* **35**, 379–384.
- STUMP, J. E. (1967). Anatomy of the normal equine foot, including microscopic features of the laminar region. *J. Am. vet. med. Ass.* **151**, 1588–1598.
- TUKEY, J. W. (1951). *Quick and Dirty Methods in Statistics*, part II, *Simple Analyses for Standard Designs*. Proc. 5th Annual Convention, Am. Soc. for Quality Control, pp. 189–197.
- WAINWRIGHT, S. A., BIGGS, W. D., CURREY, J. D. & GOSLINE, J. M. (1982). *Mechanical Design in Organisms*. Princeton, NJ: Princeton University Press.
- WILKENS, H. (1964). Zur makroskopischen und mikroskopischen Morphologie der Rinderklaue mit einem Vergleich der Architektur von Klauen- und Hufrohren. *Zentbl. Vet. Med., Ser. A* **11**, 163–234.
- WRIGHT, T. M. & HAYES, W. C. (1977). Fracture mechanics parameters for compact bone:- Effects of density and specimen thickness. *J. Biomech.* **10**, 410–430.